

Molecular Hydrogen Imaging of Star-forming Regions

S.K. Ramsay Howat¹, A. Chrysostomou², M.G. Burton³ and P.W.J.L. Brand⁴

¹ *UK ATC, Royal Observatory, Blackford Hill, Edinburgh EH9 3HJ.*

² *Joint Astronomy Centre, 660, N. A'ohoku Place, Hilo, HI 96720.*

³ *School of Physics, UNSW, Sydney, New South Wales 2052, Australia.*

⁴ *Institute for Astronomy, University of Edinburgh, Royal Observatory, Blackford Hill, Edinburgh EH9 3HJ, U.K.*

Abstract.

Observations of excited emission from molecular hydrogen have been used extensively for studies of star-forming regions for more than a decade. The characteristic response of the molecular gas to different excitation mechanisms, coupled with the in-depth theoretical modelling that has been carried out, make the near-infrared spectrum of H₂ a powerful diagnostic of the physical conditions in these regions. Early observations were able to establish whether molecular gas was excited by shocks or by radiation from young stars, using spectrometers with large beams. With improvements in theoretical understanding of the H₂ spectrum, observers were able to infer different density components within a molecular cloud from the NIR spectrum. Recent observations of the Orion Bar region made at the UK Infrared Telescope have combined Fabry-Perot imaging spectroscopy with observations at high angular resolution to examine the structure of the clouds in more detail. These observations reveal a complex filamentary structure on sub-arcsecond scales and provide direct evidence for high density clumps in the region.

1. Introduction

The observations presented in this paper are the result of an investigation of the physical structure of the Orion Bar. The aims of this project were to map the density structure in the Bar, searching for direct evidence of high density "clumps", and to investigate whether these clumps control the structure of the Bar. Our method of addressing these questions was to ratio two images of the Bar in the $v=1-0$ S(1) and $v=2-1$ S(1) emission lines of molecular hydrogen. This ratio has been shown to be sensitive to density (Burton, Hollenbach and Tielens 1990, Sternberg and Dalgarno 1989, Draine and Bertoldi 1996). In a radiatively excited cloud of density greater than a critical density of $n \sim 5 \times 10^4 \text{ cm}^{-3}$, collisions between molecular and atomic hydrogen preferentially de-excite the 2-1 S(1) line. The 1-0 S(1)/2-1 S(1) line ratio increases above the value predicted

for pure fluorescence (=1.9). In this work, this sensitivity of the line ratio to density is used as a tool to uncover the physical structure in the region. This approach has also been used by Ryder et al. (1998) in a study of Parsamyan 18.

The Orion Bar is the classic example of a photo-dissociation region (PDR), where the chemistry and physical structure are controlled by the UV radiation from young stars (see e.g. Tielens et al. 1993). Early PDR models treated such region as a slab of material of single density (Tielens and Hollenbach 1985a). Among the first observations to challenge this simple model were those of M17 SW by Stutzki & Guesten (1990) and of the Orion Bar by Parmar et al. (1991), both of which showed emission from molecular gas occurring at greater depths into the cloud than predicted. A two density component model was proposed; a low density “interclump medium” (ICM) and a number of unresolved “clumps”. Emission from the dense clumps can explain the intensity of emission from the regions, whilst allowing photons to penetrate to greater depth. Further evidence for these clumps is found in observations by Tauber et al. (1994), Hogerheijde et al. (1995), van der Werf et al. (1996) and Usuda et al. (1996), amongst others. A broad agreement on the density structure emerges from the imaging observations with 10% of the gas thought to exist in clumps with density $\sim 10^6 \text{cm}^{-3}$ embedded in a more rarified ($\sim 10^4 \text{cm}^{-3}$) ICM.

A source of continued debate is whether the clumps control structure of the Bar, or are of secondary importance compared with the interclump medium. Tauber et al. found that the barely resolved clumps in their CO data played a negligible role in determining the structure of the cloud. In contrast, van der Werf et al. (1996) concluded that the high density clumps do control the cloud structure.

Conclusions drawn from recent spectroscopic observations of H₂ emission in the NIR by Luhmann et al (1998) and Marconi et al (1998) are at odds with each other and with the conclusions of the imaging studies. Luhman et al find that the spectrum can be modelled by a single high density component ($\sim 10^6 \text{cm}^{-3}$). Marconi et al. find no evidence for densities higher than $\sim 10^4 \text{cm}^{-3}$. Both groups confirm the conclusion of Burton et al. (1991) that there is no evidence for shock excitation in the NIR emission spectrum of H₂.

To a greater or lesser extent, each of these studies suffers from beam dilution effects. By observing the Bar at high angular resolution, we aimed to resolve the clumps on sub-arcsecond scales and to clarify the importance of a two clump model in characterising the Orion Bar.

2. Observations

The observations were made with the UKIRT telescope on 1998 January 16-19. The infrared camera, IRCAM was used with a pixel scale of 0.286 arcsec and a 72 arcsec field of view. The field was centred on the position selected by Hayashi et al (1985). A 350kms^{-1} Fabry-Perot etalon from Queensgate instruments was used to isolate the lines. In a region with such a high line-to-continuum ratio, the rejection of continuum from the line pass-band is important to maximise signal/noise on the line flux. The method of observing was to observe the line, off-set to sky, re-tune the FP to nearby continuum, observe the continuum then offset to sky and make a measurement of the sky at the continuum wavelength.

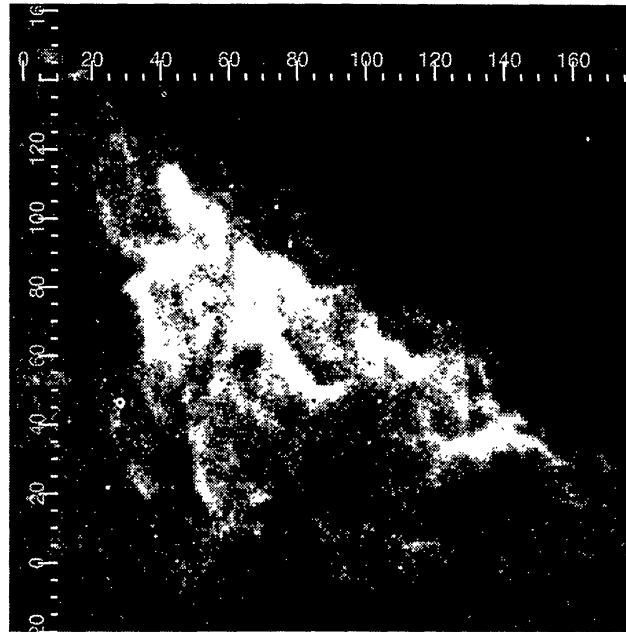


Figure 1. The 1-0 S(1) line of H₂ imaged using a Fabry-Perot.

A quarter of the total observing time is spent observing the source. Over the four nights, the 1-0 S(1) was observed for 45mins and the 2-1 S(1) line for 2hours and 30mins. Frames were “jittered” by 5arcsecs as well as offset to the sky. In the reduction, each frame was divided by a flat-field frame derived from the median of the sky observations. The flat-field frame used was specific to the FP setting. Individual frames were registered using the many field stars present before constructing the final mosaic. The 1-0 S(1) and 2-1 S(1) images are shown in Figures 1 & 2.

3. Discussion and analysis

The images reveal a complex filamentary structure on scales as small as 0.5arc-sec (equivalent to 10^{-3} pc). Comparing the $v=1-0$ S(1) and $v=2-1$ S(1) frames, changes in the relative intensity are seen, providing immediate evidence for changing densities across the region. For example the northernmost filament running parallel to the Bar ((40,115) - (50,110) using the coordinates in Figure 1) is the brightest 1-0 S(1) feature. The brightest 2-1 S(1) feature is centred on (40,90).

A contour plot of the ratio of the two line frames is shown in Figure 3. The line images were placed on the same reference frame and were smoothed to increase the signal/noise in the 2-1 S(1) image before ratioing. Typical values of the ratio, line intensity and implied density for the brightest structures in the region are given in Table 1. The density has been derived from the models of Draine and Bertoldi (1996), assuming an intensity of the UV field for the region of 5×10^4 larger than that of the ISM (Tielens and Hollenbach 1985b).



Figure 2. The 2-1 S(1) line of H₂ imaged using a Fabry-Perot.

The areas where the density is highest are immediately apparent as two bright ridges running from (40,120)-(50,110) and (30,90)-(40,60), using coordinates from Figure 3. The filament bridging these features, (60,110)-(30,90), is fainter in the ratio map, despite being prominent in the 1-0 S(1) intensity map. The filaments are surrounded by gas with a line ratio of ~ 3 , a value typical of low density fluorescence, though this must be interpreted cautiously as the signal/noise on the 2-1 S(1) line is low in many of these regions.

The anti-correlation between changes in intensity and density can be understood as follows. As the density increases, collisional de-excitation occurs for both the $v=1$ and $v=2$ levels, but the effect is stronger for the $v=2$ levels. In addition, the $v=1$ -0 S(1) line may also be collisionally excited. Hence the line ratio tends to increase with increasing density, and may be expected to be correlated with increasing 1-0 S(1) line strength. However, the flux per pixel depends on the volume of gas present in the pixel, as well as on the density of the gas. If the clumps in the region were fully resolved, the changes in intensity and line ratio would be correlated. Where a high density region is of low intensity, the pixels contain unresolved clumps. This highlights the power of the approach taken here, where the density is measured directly rather than inferred from changing line intensity. Regions of high and low density are indistinguishable in a single line map.

For the whole area observed, the line ratio has been calculated and compared with the 1-0 S(1) line strength. Only those pixels with signal-to-noise on the 2-1 S(1) line of greater than 5 were selected. Ratios in the range $1 \leq 1-0 \text{ S}(1)/2-1 \text{ S}(1) \leq 8$ are measured. The low ratios are consistent with pure fluorescent emission, with no thermal contribution to the spectrum. This is emission from

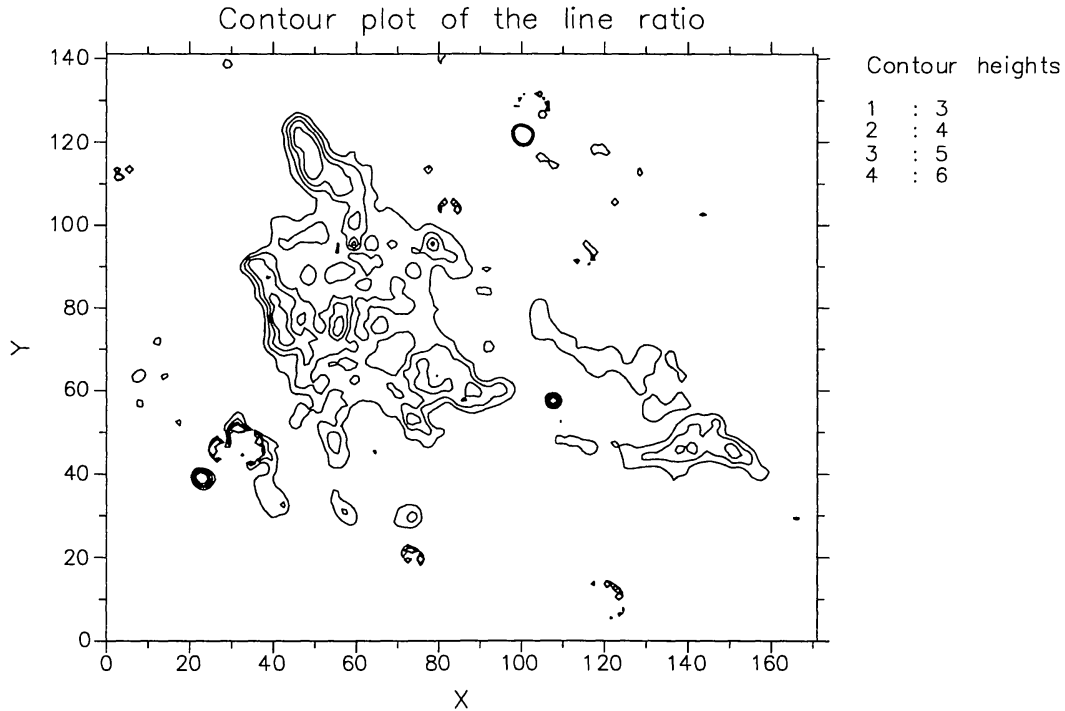


Figure 3. A contour plot of the line ratios in the Orion Bar.

the ICM with density $\leq 10^4 \text{cm}^{-3}$. Measured ratios of ~ 8 imply the presence of densities greater than 10^6cm^{-3} , as required to explain the observed CO 1-0/7-6 and CO 7-6/14-13 ratios from Tauber et al. (1994) and Stacey et al. (1993).

(x,y) from Figure 3	$I_{\text{H}_2} \nu=1-0 \text{ S}(1)$ $\text{Wm}^{-2}\text{arcsec}^{-2}$	$I_{\text{H}_2} \nu=2-1 \text{ S}(1)$ $\text{Wm}^{-2}\text{arcsec}^{-2}$	ratio	density
(40,120)-(50,110)	$\geq 6 \times 10^{-18}$	1×10^{-18}	6 ± 0.6	10^6cm^{-3}
(60,110)-(30,90)	4.5×10^{-18}	1.25×10^{-18}	3.5 ± 0.4	10^5cm^{-3}
(30,90)-(40,6)	3×10^{-18}	0.5×10^{-18}	6 ± 1.2	10^6cm^{-3}

Table 1. Example line strengths and line ratios from prominent filaments in the Bar maps.

Since these data reveal the high density clumps, they can be used to estimate whether the clumps we observe are responsible for the structure of the Bar more effectively than previous data sets. The ICM density is taken as 10^4cm^{-3} . Using the column density for H_2 of $5 \times 10^{21} \text{cm}^{-2}$ as derived from the CO observations of Tauber et al. and a distance to the Bar of 460pc, an optical depth of $1A_\nu$ should correspond to 70arcsecs. Tielens & Hollenbach (1985a) show that the H_2 peak occurs at an optical depth of ~ 2 , or 140arcsecs into the cloud in the case of the Orion Bar. We see the H_2 emission peak at a distance of 15arcsecs from the ionisation front. This implies that a higher density gas component is controlling the structure of the cloud. The dense filaments of H_2 emission cover an area of approximately 125arcsecs squared or a projected area of $\sim 45\%$ of the Bar.

Assuming that the filling factor is the same along the line of sight, the volume filling factor is 20%, and the clumps are a significant fraction of the cloud. Our data therefore support the conclusion of van der Werf et al. that the clumps control the cloud structure.

4. Conclusions and Prospects

Pseudo-3D spectroscopy of the Orion Bar using Fabry-Perot imaging in key molecular transitions has provided a picture of the density structure of the Orion Bar. Filaments with densities in the range 10^5cm^{-3} to 10^6cm^{-3} are observed and the interclump medium ($n \sim 10^4\text{cm}^{-3}$) detected. The structure of the Bar is found to be controlled by these high density clumps.

FP imaging provided the excellent spatial coverage required to survey this nearby region. Follow-up studies in this and other PDRs will benefit from the development of true 3D spectroscopy via a NIR integral field unit such as that being developed for the UKIRT Imaging Spectrometer, UIST (Wells, Hastings and Ramsay Howat 2000). FP imaging requires 75% of the observing time to be spent on calibrations. This experiment, requiring a total integration time of 13 hours, could be completed in approximately one hour.

UKIRT is operated by the Joint Astronomy Centre on behalf of the UK Particle Physics and Astronomy Research Council. The authors would like to thank Thor Wold for his assistance at the telescope.

References

- Burton, M.G., Hollenbach, D.J. & Tielens, A.G.G.M. 1990, *ApJ*, 365, 620.
Draine, B.T. & Bertoldi, F. 1996, *ApJ*, 468, 269.
Hayashi, M., Hasegawa, T., Gatley, I., Garden, R., Kaifu, N., 1985, *MNRAS*, 215, 31.
Luhmann, K.L., Engelbracht, C.W. & Luhman, M.L. 1998, *ApJ*, 499, 799.
Marconi, A., Testi, L., Natta, A. & Walmsley, C.M. 1998, *A&A*, 330, 696.
Parmar, P.S., Lacy, J.H. & Achtermann, J.M., 1991, *ApJ*, 372, L25.
Hogerheijde, M.R., Jansen, D.J. & van Dishoeck, E.F. 1995, *Astron. Astrophys.*, 294, 792.
Ryder, S.D., Allen, L.E., Burton, M.G., Ashley, M.C.B. & Storey, J.W.V. 1998, *MNRAS*, 294, 338.
Stacey, G.F., Jaffe, D.T., Geis, N., Genzel, R. Haris, A.I., Poglitsch, A., Stutzki, J. & Townes, C.H., 1993, *Ap.J.*, 404, 219
Sternberg, A. & Dalgarno, A., 1989, *ApJ*, 338, 197.
Stutzki, J. & Guesten, R. 1990, *ApJ*, 20, 513.
Tauber, J.A., Tielens, A.G.G.M., Meixner, M., and Goldsmith, Paul F., 1994, *Ap.J.*, 422, 136.
Tielens, A.G.G.M. & Hollenbach, D. 1985a, *Ap.J.*, 291, 722.
Tielens, A.G.G.M. & Hollenbach, D. 1985b, *Ap.J.*, 291, 747.
Tielens, A.G.G.M., Meixner, M.M., van der Werf, P.P., Bregman, J., Tauber, J.A., Stutzki, J., & Rank, D., 1993, *Science*, 262, 86.
Usuda, T., Sugai, H., Kawabata, H., Inoue, M., Kataza, H. & Tanaka, M. 1996, *ApJ*, 464, 818.
Van der Werf, P.P., Stutzki, J., Sternberg, A., & Krabbe, A. 1996, *Astron. Astrophys.*, 313, 633.
Wells, M., Hastings, P.R. & Ramsay Howat, S.K. 2000, this volume.